

Compact Filtering Power Divider Based on Half Mode Substrate Integrated Waveguide

Ali-Reza Moznebi and Kambiz Afrooz*

Abstract—In this paper, a compact filtering power divider (PD) based on half mode substrate integrated waveguide (HMSIW) is presented. The proposed structure is realized by etching slots on the top layer of the HMSIW PD. Accordingly, two resonators are embedded in each patch, as a second order filter. The slots dimensions are obtained by the relationship between them and the extracted external quality factor and coupling coefficient. A good agreement between the simulated and measured results is reported. The measured 3 dB fractional bandwidth is 25% (6.3–8.1 GHz). The maximum insertion loss is 0.9 dB, and the return loss is above 20 dB in the passband. This design has the advantages of low insertion loss, improved out-of-band rejection, compact size, controllable bandwidth, and high selectivity.

1. INTRODUCTION

Conventional waveguides are extensively used in many microwave and millimeter-wave systems such as power dividers (PDs) and high Q filters because of their high power capacity and low loss [1, 2]. However, their applications are limited due to large volume and high cost [3]. Recently, substrate integrated waveguide (SIW) structure has been introduced [4, 5]. An SIW is arranged by two rows of metallic via holes in a planar substrate having the benefits of the conventional waveguides, compactness in size, low cost, and easy integration with planar circuits [6]. The size of an SIW is relatively large. The concept of the half mode substrate integrated waveguide (HMSIW) has been presented in [7]. In this configuration, a bisecting plane is inserted along the magnetic wall. Compared to an SIW, the HMSIW solution allows a size reduction about 50%, as shown in Figure 1.

Bandpass filters can be used for frequency selection and suppression of unwanted bands. In the past few years, increased attention has been paid to the implementation of bandpass filters with the SIW technique [8, 9]. In [8], a dual-band SIW resonator with Sierpinski fractal geometry is proposed. This paper shows an interesting technique to reduce the size of the SIW structure. However, this design has the disadvantage of narrow operation bandwidth due to the resonant nature of its configuration. In [9], a HMSIW filter is introduced, and compact size and controllable bandwidth are obtained. Newly, the combination of the power dividing and filtering functions into a single device is taken into consideration. The combination of both functionalities provides a circuit with benefits of low loss, low cost, and compact size. Several PDs based on SIW and HMSIW have been investigated [10–17]. However, the proposed circuits in [10–14] do not include the bandpass filtering response, which restricts their applications in practical systems. In [15], a multilayer SIW PD with bandpass-filtering response is reported. To achieve bandpass response, four inductive posts are added to the multilayer SIW PD. However, this kind of power divider has the disadvantages of large size and narrow operating bandwidth. An out-of-phase filtering PD using a rectangular SIW cavity is proposed in [16]. This circuit uses magnetic coupling by via-hole coupling window and has large size. In [17], a PD integrated with SIW and defected ground

Received 8 April 2016, Accepted 30 June 2016, Scheduled 12 July 2016

* Corresponding author: Kambiz Afrooz (afrooz@uk.ac.ir).

The authors are with the Department of Electrical Engineering, Shahid Bahonar University of Kerman, Kerman, Iran.

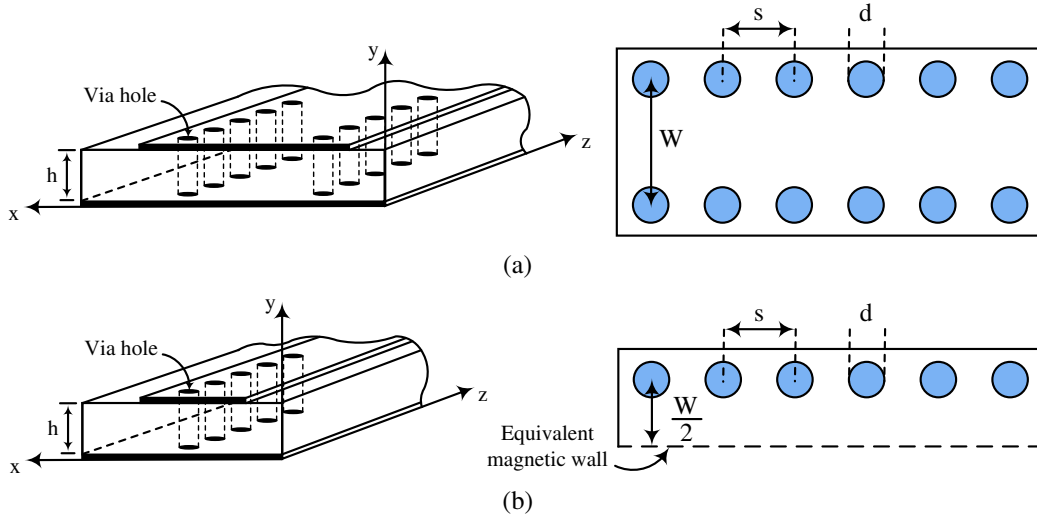


Figure 1. Configuration of a: (a) SIW structure; (b) HMSIW structure.

structures (DGS) techniques is presented. The reported filtering PDs in [15–17] are not proper to design at high frequencies due to the limitation of via-holes fabrication [18].

In this paper, an HMSIW PD prototype with a bandpass filter response is designed, simulated, and fabricated. A part of the HMSIW between two rectangular slots is considered as a resonator [9]. Here, two resonators are embedded by etching three rectangular slots on the top layer of each patch. The coupled resonators give the bandpass function. This design has the advantages of low insertion loss, improved out-of-band rejection, compact size, controllable bandwidth, and high selectivity. In this structure, the bandwidth can be controlled by the transverse slots. Figure 2 shows the configuration of the HMSIW PD and proposed filtering HMSIW PD. The paper is organized as follows: Section 1, the introduction; Section 2, the design procedure and results of the HMSIW PD; Section 3, the design procedure and results of the filtering HMSIW PD; Section 4, the conclusion.

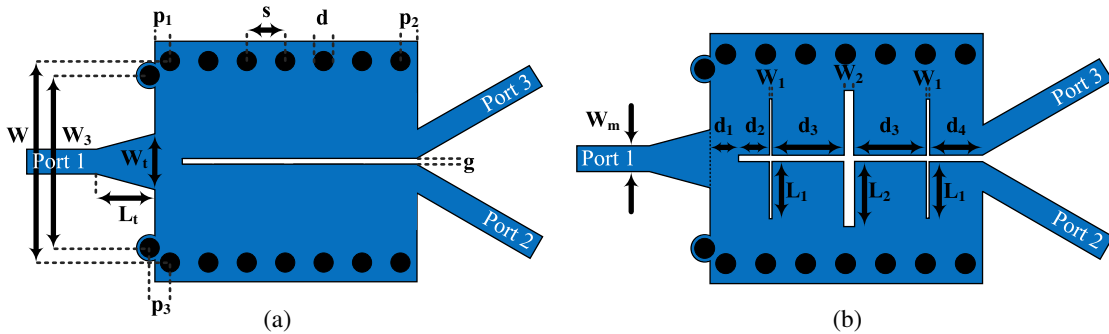


Figure 2. Configuration of the: (a) HMSIW PD; (b) proposed filtering HMSIW PD.

2. HALF MODE SUBSTRATE INTEGRATED WAVEGUIDE POWER DIVIDER

2.1. Design Procedure

The methodology in this section is divided into two steps. Step 1: calculating the basic SIW parameters. Step 2: determining the taper-via transition parameters.

The SIW structure is a quasi-rectangular waveguide. In this structure, only TE_{n0} modes can propagate, and TM modes cannot be guided due to the dielectric gaps created by the via separations [19].

The dominant mode of this structure is TE₁₀. By using the formula obtained in [20], the equivalent width of the SIW (W_{eff}) is equal to:

$$W_{eff} = W - 1.08 \frac{d^2}{s} + 0.1 \frac{d^2}{W} \quad (1)$$

The cut-off frequency of the SIW can be calculated by the following formula [21]:

$$f_{c10} = \frac{c}{2W_{eff} \sqrt{\mu_r \epsilon_r}} \quad (2)$$

In Equations (1) and (2), W is the width of the SIW, d the diameter of the vias, s the distance between the center of two adjacent vias, c the light velocity in vacuum, ϵ_r the relative permittivity of the substrate, and μ_r the relative permeability of the substrate. For better performance of the circuit, d and s are limited as follows [22]:

$$\frac{s}{d} \leq 2 \quad (3)$$

In the input, a microstrip-to-SIW transition is used [23]. It features two vias, which have the same diameter as the SIW vias and are located symmetrically at both sides of the microstrip taper. The taper-via transition parameters can be calculated as:

$$\begin{aligned} L_t &= 0.2368 \lambda_{gMS} \\ W_t &= W_m + 0.1547W \\ p_3 &= 0.6561s \\ W_3 &= 0.8556W \end{aligned} \quad (4)$$

where W_m is the width of 50 Ohm microstrip line and λ_{gMS} the guided wavelength of microstrip line calculated at the center frequency:

$$\lambda_{gMS} = \frac{\lambda_{g0}}{\sqrt{\epsilon_{reff}}} \quad (5)$$

where ϵ_{reff} refers to the effective dielectric constant of the microstrip line and λ_{g0} the wavelength in free space. To achieve the HMSIW PD, the SIW which has the highpass characteristic is divided into two HMSIWPs.

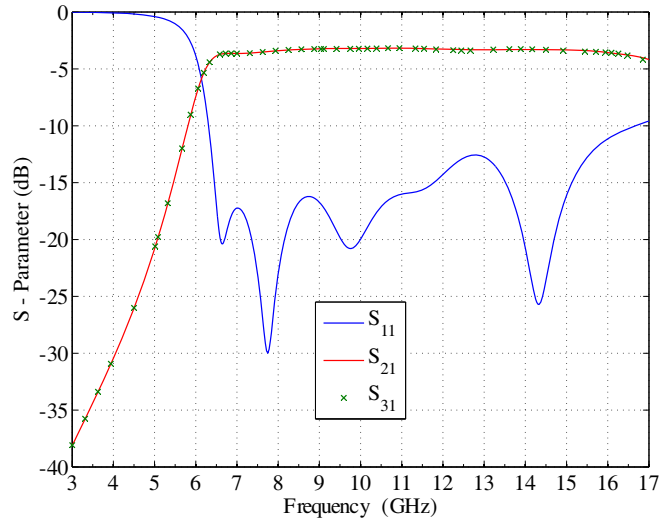


Figure 3. Simulated S_{11} , S_{21} , and S_{31} of the HMSIW PD.

2.2. Results

The HMSIW PD is simulated on a single layer Rogers RO4003C substrate with a thickness, relative permittivity, and loss tangent of 0.8128 mm, 3.55, and 0.0027, respectively. The simulated results of this PD are shown in Figure 3. In the aforementioned HMSIW PD, the return loss is greater than 15 dB over 6.45 to 11.75 GHz (fractional bandwidth of 58%), and the maximum insertion loss is 0.9 dB in the passband.

3. FILTERING HALF MODE SUBSTRATE INTEGRATED WAVEGUIDE POWER DIVIDER

3.1. Design Procedure

The mentioned HMSIW PD is transformed to the filtering HMSIW PD to improve the performance of the circuit. To design the filtering HMSIW PD, the adjusted transverse slots are added to the HMSIW PD. Each part of the HMSIW between two transverse slots is considered as a resonator. Here, two resonators are embedded by etching three rectangular slots on the top layer of each patch. The coupled resonators give the bandpass function. The coupling scheme of this filtering PD is illustrated in Figure 4. A bandpass filter is designed to meet the specifications: the center frequency $f_0 = 7$ GHz and 3 dB bandwidth $BW = 1.2$ GHz with 0.5 dB passband ripple. This design consists of two steps.

Step 1: The external quality factor (Q_e) and coupling coefficient between the two resonators (K_{12}) can be evaluated by using the following relations [24]:

$$Q_e = \frac{g_0 g_1 f_0}{BW} \quad (6)$$

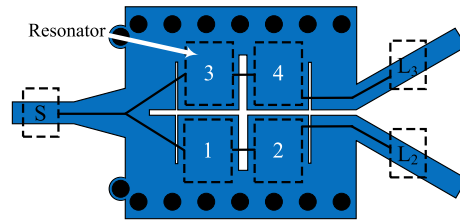


Figure 4. Coupling scheme of the proposed filtering HMSIW PD.

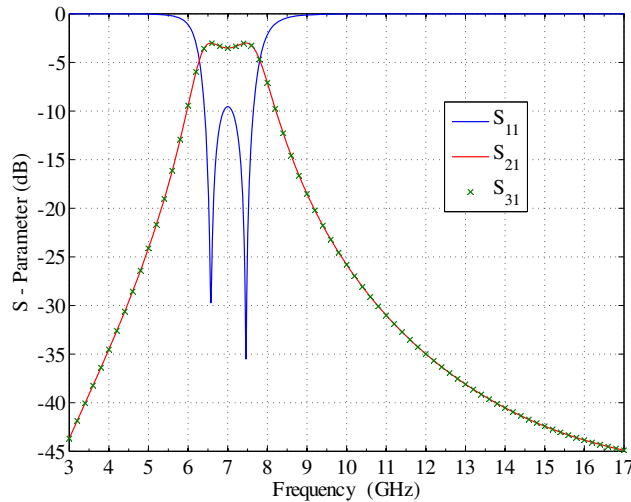


Figure 5. Ideal response of the designed bandpass filter.

$$K_{12} = \frac{BW}{f_0\sqrt{g_1g_2}} \tag{7}$$

where $g_0, g_1, g_2,$ and g_3 are Chebyshev low-pass prototype element values. The evaluated value of Q_e is 8.18, and K_{12} is 0.172. The ideal response for this filter is shown in Figure 5.

Step 2: The width and length of the rectangular slots are tuned by a 3D EM simulator to determine the relationship between the physical dimensions of the slots and Q_e and K_{12} . Q_e and K_{12} can be calculated by [24]:

$$Q_e = \frac{2f_0}{BW} \tag{8}$$

$$K_{12} = \frac{f_1^2 - f_2^2}{f_1^2 + f_2^2} \tag{9}$$

where f_1 and f_2 represent the higher and lower resonant frequencies, respectively. Figure 6 shows the external quality factor and coupling coefficient between the two resonators versus the width and length of the rectangular slots. The external quality factor and coupling coefficient can be increased by

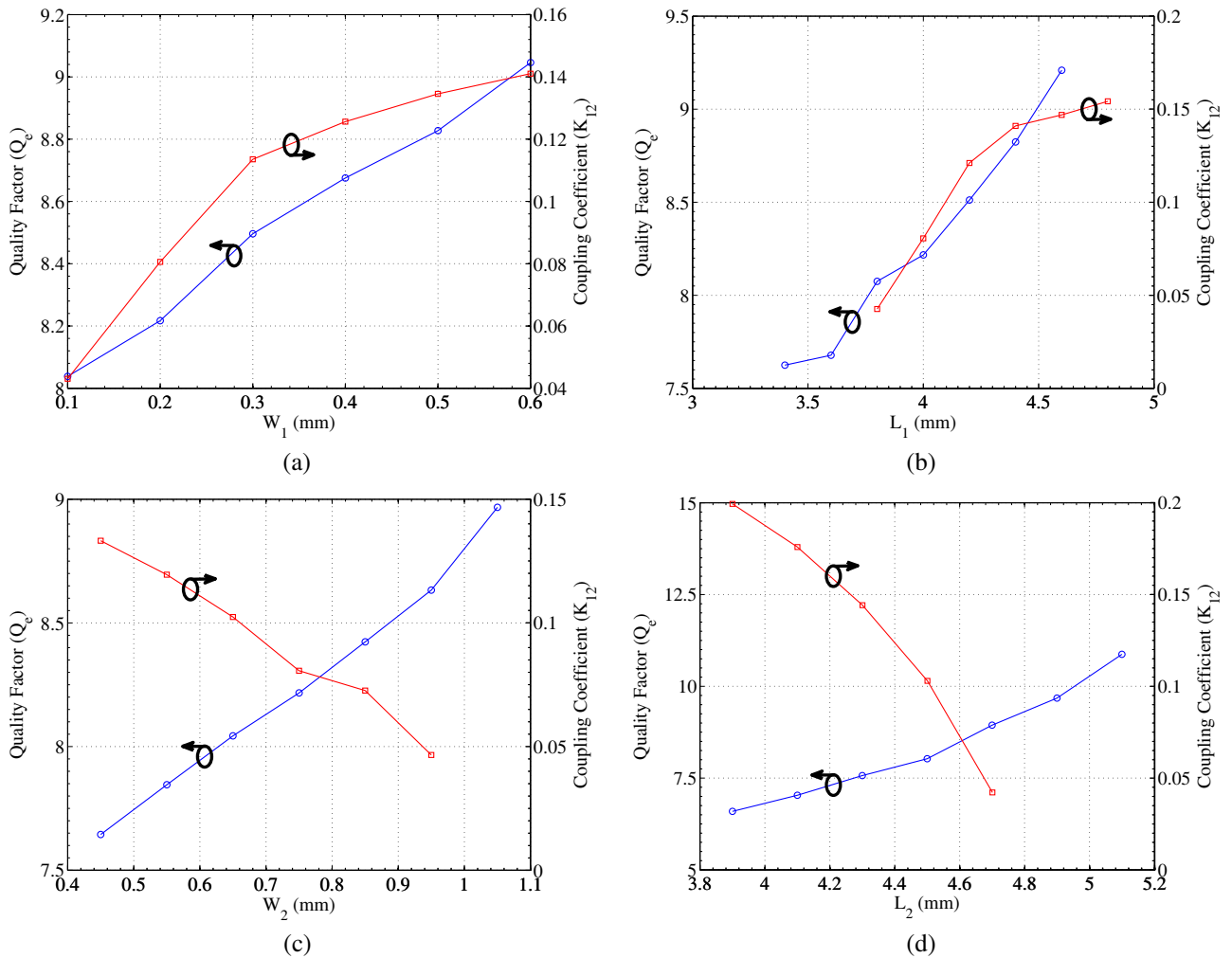


Figure 6. Extracted Q_e and K_{12} versus different: (a) W_1 when $L_1 = 4$ mm, $W_2 = 0.75$ mm, and $L_2 = 4.58$ mm; (b) L_1 when $W_1 = 0.2$ mm, $W_2 = 0.75$ mm, and $L_2 = 4.58$ mm; (c) W_2 when $W_1 = 0.2$ mm, $L_1 = 4$ mm, and $L_2 = 4.58$ mm; (d) L_2 when $W_1 = 0.2$ mm, $L_1 = 4$ mm, and $W_2 = 0.75$ mm.

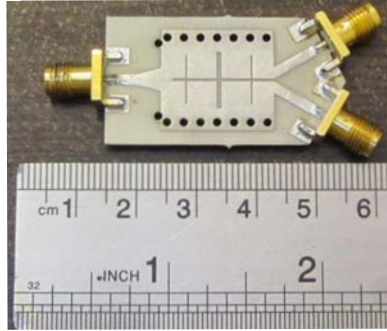
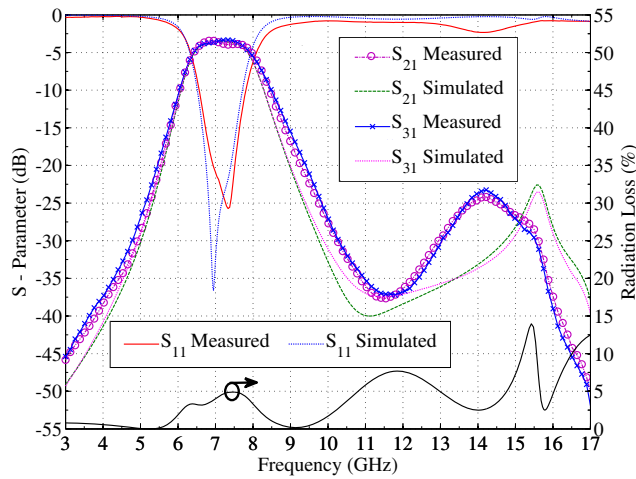
Table 1. Dimensions of the HMSIW PD and filtering HMSIW PD.

W	14.65 (mm)	L_2	4.58 (mm)	p_1	1.11 (mm)
W_1	0.2 (mm)	L_t	4.24 (mm)	p_2	1.22 (mm)
W_2	0.75 (mm)	d_1	2 (mm)	p_3	1.04 (mm)
W_3	12.56 (mm)	d_2	2.15 (mm)	s	2.79 (mm)
W_t	4.06 (mm)	d_3	5.02 (mm)	d	1.45 (mm)
L_1	4 (mm)	d_4	3.74 (mm)	g	0.4 (mm)

increasing W_1 and L_1 , as shown in Figure 6(a) and Figure 6(b). Moreover, Q_e can be increased, and K_{12} can be decreased by increasing W_2 and L_2 , as shown in Figure 6(c) and Figure 6(d). It should be noted here that the extracted Q_e and K_{12} from Figure 5 are 8.2 and 0.126, respectively. Table 1 exhibits the dimensions of the HMSIW PD and filtering HMSIW PD.

3.2. Results

The filtering HMSIW PD is fabricated on a single-layer Rogers RO4003C substrate with a thickness, relative permittivity, and loss tangent of 0.8128 mm, 3.55, and 0.0027, respectively. A photograph of the proposed filtering HMSIW PD is depicted in Figure 7. The fabricated circuit is tested by the network analyzer ‘‘Rohde & Schwarz, zvk’’. Figure 8 indicates the simulated and measured S_{11} , S_{21} , and S_{31} .

**Figure 7.** Photograph of the fabricated filtering HMSIW PD.**Figure 8.** Measured and simulated S_{11} , S_{21} , and S_{31} of the filtering HMSIW PD.

The measured 3 dB fractional bandwidth is 25% (6.3–8.1 GHz). The maximum insertion loss is 0.9 dB, and the return loss is above 20 dB in the passband. Moreover, the out-of-band rejection band is over 25 dB from 9.8 GHz to 13.7 GHz. The simulated and measured results are in good agreement. There is a slight frequency shift of approximately 2%, and the maximum simulated insertion loss is about 0.3 dB better than the measured insertion loss. Some slight differences between the simulated and measured results are mainly caused by the insertion loss of SMA connectors and the tolerances of the dielectric constant. In Figure 8, the radiation loss is defined as:

$$R_r = 1 - S_{11}S_{11}^* - S_{21}S_{21}^* - S_{31}S_{31}^* \quad (10)$$

In this figure, the radiation loss (R_r) is less than 4.9% under the conditions of lossless metal and substrate. This parameter guarantees that the produced radiation is negligible. In Table 2, a comparison between the presented filtering HMSIW PD and the other PDs is summarized. In this table, the advantages in fractional bandwidth and insertion loss are very obvious. Furthermore, the proposed filtering HMSIW PD has a size of $1.04 \times 0.78\lambda_g^2$, which is much more compact than that in [14–17]. Also, compared with the reported circuit in [17], a size reduction of 42% is achieved.

Table 2. Comparison with other PDs.

Reference	Size (λ_g^2)	Frequency Response	3 dB Fractional Bandwidth (%)	Insertion Loss (dB)
[14]	3.91×1.64	No	8.47 (15 dB Return Loss)	< 1.5
[15]	0.88×4.08	Yes	4.8	< 1
[16]	0.65×5.05	Yes	13.83	< 1.4
[17]	1.15×1.65	Yes	16	< 1.2
This work	0.78×1.04	Yes	25	< 0.9

4. CONCLUSION

A compact filtering PD based on HMSIW has been presented. The bandpass filtering response is implemented by etching slots on the top layer of the HMSIW PD. The slots dimensions are obtained by the relationship between them and the extracted external quality factor and coupling coefficient. The presented circuit has been designed, fabricated, and measured. A good agreement can be found between the simulated and measured results over the operating frequency range. This structure has the advantages of low insertion loss, improved out-of-band rejection, compact size, controllable bandwidth and high selectivity. Compared with the previously reported circuits, this filtering HMSIW PD can be widely used in microwave and millimeter-wave systems because of its simplicity and compactness. The isolation among output ports of this filtering PD can be obtained in the future work.

REFERENCES

1. Chen, X. P. and K. Wu, "Substrate integrated waveguide filter: Basic design rules and fundamental structure features," *IEEE Microw. Magazine*, Vol. 15, No. 5, 108–116, 2014.
2. Rui, M., L. Mengjia, S. Houjun, L. Zhen, and Z. Pei, "Design and simulation of a W-band two-way power divider based on substrate integrated waveguide," *IEEE International Conference on Microw. Technology & Computational Electromagnetics (ICMTCE)*, 100–102, 2013.
3. Hao, Z., W. Hong, H. Li, H. Zhang, and K. Wu, "Multiway broadband substrate integrated waveguide (SIW) power divider," *Antennas and Propagation Society Int. Symp.*, Vol. 1, 639–642, 2005.
4. Uchimura, H., T. Takenoshita, and M. Fujii, "Development of a laminated waveguide," *IEEE Trans. Microw. Theory Tech.*, Vol. 46, No. 12, 2438–2443, 1998.
5. Yan, L., W. Hong, K. Wu, and T. J. Cui, "Investigations on the propagation characteristics of the substrate integrated waveguide based on the method of lines," *IEE Proc. Microw. Antennas Prop.*, Vol. 152, No. 1, 35–42, 2005.

6. Bozzi, M., A. Georgiadis, and K. Wu, "Review of substrate-integrated waveguide circuits and antennas," *IET Microw. Antennas Prop.*, Vol. 5, No. 8, 909–920, 2011.
7. Hong, W., B. Liu, Y. Wang, Q. Lai, H. Tang, X. X. Yin, Y. D. Dong, Y. Zhang, and K. Wu, "Half mode substrate integrated waveguide: A new guided wave structure for microwave and millimeter wave application," *Proc. Joint 31st Int. Conf. Infr. Millim. Waves and 14th Int Conf. Terahertz Electron.*, 219–219, 2006.
8. Chiapperino, M. A., O. Losito, T. Castellano, G. Venanzoni, L. Mescia, G. Angeloni, C. Renghini, P. Carta, P. Potenza, and F. Prudenzano, "Dual-band substrate integrated waveguide resonator based on Sierpinski carpet," *Progress In Electromagnetics Research C*, Vol. 57, 1–12, 2015.
9. Wang, Y., W. Hong, Y. Dong, B. Liu, H. J. Tang, J. Chen, X. Yin, and K. Wu, "Half mode substrate integrated waveguide (HMSIW) bandpass filter," *IEEE Microw. Wirel. Compon. Lett.*, Vol. 17, No. 4, 265–267, 2007.
10. Zhang, Z. Y. and K. Wu, "Broadband half-mode substrate integrated waveguide (HMSIW) Wilkinson power divider," *IEEE MTT-S Int. Microw. Symp. Dig.*, 879–882, 2008.
11. Jin, H. and G. Wen, "A novel four-way Ka-band spatial power combiner based on HMSIW," *IEEE Microw. Wirel. Compon. Lett.*, Vol. 18, No. 8, 515–517, 2008.
12. Smith, N. A. and R. Abhari, "Compact substrate integrated waveguide Wilkinson power dividers," *IEEE International Symposium on Antennas and Propagation*, 1–4, 2009.
13. Zou, X., C. M. Tong, and D. W. Yu, "Y-junction power divider based on substrate integrated waveguide," *Electron. Lett.*, Vol. 47, No. 25, 1375–1376, 2011.
14. Kim, K., J. Byun, and H.-Y. Lee, "Substrate integrated waveguide Wilkinson power divider with improved isolation performance," *Progress In Electromagnetics Research Letters*, Vol. 19, 41–48, 2010.
15. Hui, J. N., W. J. Feng, and W. Q. Che, "Balun bandpass filter based on multilayer substrate integrated waveguide power divider," *Electron. Lett.*, Vol. 48, No. 10, 571–573, 2012.
16. Zhang, X., H. Wang, C. Yu, Q. Wu, and W. Hong, "Out-of-phase filtering power divider using rectangular SIW cavity," *Microwave Conference (APMC)*, 705–707, 2014.
17. He, Z., J. Cai, Z. Shao, X. Li, and Y. Huang, "A novel power divider integrated with SIW and DGS technology," *Progress In Electromagnetics Research*, Vol. 139, 289–301, 2013.
18. Wong, S. W., K. Wang, Z. N. Chen, and Q. X. Chu, "Design of millimeter-wave bandpass filter using electric coupling of substrate integrated waveguide (SIW)," *IEEE Microw. Wirel. Compon. Lett.*, Vol. 24, No. 1, 26–28, 2014.
19. Rayas-Sanchez, J. E. and V. Gutierrez-Ayala, "A general EM-based design procedure for single-layer substrate integrated waveguide interconnects with microstrip transitions," *IEEE MTT-S Int. Microw. Symp. Dig.*, 983–986, 2008.
20. Xu, F. and K. Wu, "Guided-wave and leakage characteristics of substrate integrated waveguide," *IEEE Trans. Microw. Theory Tech.*, Vol. 53, No. 1, 66–73, 2005.
21. Pozar, D. M., *Microwave Engineering*, Wiley, New York, 2011.
22. Wu, K., D. Deslandes, and Y. Cassivi, "The substrate integrated circuits — A new concept for high-frequency electronics and optoelectronics," *Telecommun. Modern Satellite, Cable, Broadcast. Service/TELSIKS 6th Int. Conf.*, Vol. 1, P-III–P-X, 2003.
23. Kordiboroujeni, Z. and J. Bornemann, "New wideband transition from microstrip line to substrate integrated waveguide," *IEEE Trans. Microw. Theory Tech.*, Vol. 62, No. 12, 2983–2989, 2014.
24. Hong, J. S. and M. J. Lancaster, *Microstrip Filters for RF/Microwave Applications*, Wiley, New York, 2004.